IMA Journal of Applied Mathematics (2022) Page 1 of 31
doi:10.1093/imamat/dri017

Temporal instability of curved viscous fibers with a radial electric field

ABDULLAH M ALSHARIF[1*] AND EMILIAN I. PĂRĂU[2]

[1] *Department of Mathematics and statistics, College of Science, Taif University, P. O. Box 11099, Taif 21944, Saudi Arabia.*

[2] *School of Mathematics, University of East Anglia, Norwich NR4 7TJ, UK.*

[*] *Corresponding author: a.alshrif@tu.edu.sa*

[Received on 11 February 2021]

[Received on 2 February 2022]

One-dimensional equations are derived for a rotating viscous slender liquid jet in a radial electric field using asymptotic methods. The trajectory of the curved Newtonian liquid jets is found by solving the nonlinear one-dimensional equations. The temporal instability of the steady solutions is analysed. It was found that the electric force enhances the growth rate and increases its corresponding maximum wavenumber.

Keywords: linear instability, liquid jets, electric field

1. Introduction

The study of the trajectory and the breakup of liquid jets has a long history (see Eggers (1997, 2008) for reviews), with many engineering and industrial applications. The linear theory of incompressible inviscid liquid straight jets was derived analytically by Rayleigh (l878), who discovered that the surface tension is responsible for the linear instability. Later, Weber (1931) extended the linear instability theory of liquid jets by considering the effect of the viscosity. In particular, he found that the viscosity increases the wavelength of the most unstable modes.

In the last decades many authors have also considered the stability of curved viscous liquid jets, by performing experiments (e.g. Wong et al. (2004), Hawkins et al. (2010) and Partridge et al. (2005)) or undertaking analytical studies (e.g. Yarin (1993), Wallwork (2002), Decent et al. (2002)). These studies on instability of curved liquid jets have been extended by considering a variety of non-Newtonian fluids, such as power law fluids or polymers (e.g. Divvela et al. (2017), Alsharif (2019), Taghavi and Larson (2014), Alsharif et al. (2015), Noroozi et al.(2017) and Riahi (2017)). The study of curved liquid jets which can be obtained by centrifugal jet spinning (CJS) (also called sometimes forcespinning FS) was in part motivated by a variety of academic and engineering applications, such as as ink-jet printers Tomiat et al. (1986), fuel spraying Jones et al. (1971), microencapsulation and electro-spinning Doshi et al. (1993) and Shin et al. (2001). The production in the last decades of nanofibers for industrial applications by applying electric fields has spanned new works which were interested in understanding the effect of electric field on the trajectories of liquid jets and their stability (Reneker el al. (2000), Hohman et al. (2001a, 2001b) and Yarin et al. (2001), Feng (2003)).

More recently, experiments have been performed by combining the effects of forcespinning with electrospinning (e.g. Chang et al. (2014), Liao et al. (2011a), (2011), Dabirian et al. (2013), Hashemi et al. (2018)). By combining these two techniques better-quality uniform nanofibers are obtained, by removing the whipping instability observed when only the electrospinning was used on viscoelastic flu-

ids. There are very few theoretical results on the combined effect of forcespinning with electrospinning on Newtonian and non-Newtonian jets, and they are focussed on steady state results (e.g. Hashemi et al. (2018), Riahi (2019)).

In this paper we investigate theoretically the combined effect of forcespinning and electrospinning on viscous liquid jets. The trajectory and the temporal linear instability of slender curved viscous jets on a radial electric field are studied by extending the works of Wallwork et al (2002), Părău et al. (2006, 2007). This provides useful information about regimes of physical parameters such as viscosity, rotation rate, electric field strength, conductivity of the fluids where instabilities can be avoided or minimized. Moreover, a better understanding of the forcespinning/electrospinning process will inform future studies of more applied problems, where non-Newtonian liquids will be considered and experimental and theoretical results will be compared.

The governing equations and the dimensionless parameters are introduced in Section 2 and 3 (see also Appendix). We use the asymptotic analysis of the slender jet to derive a set of one-dimensional equations (Wallwork (2002), Decent et al. (2018)) in Section 4. In Section 5 we solve the steady equations obtained and calculate the steady state solutions of viscous liquid jets in centrifugal spinning with a radial electric field. Typical values of parameters used in some experiments are also presented in this Section. By perturbing these steady solutions, we perform a temporal stability analysis in Section 6. We derive the dispersion relation and solve it to examine the behaviour of some parameters on the linear instability of centrifugal jet spinning with electric field. The paper finishes with a discussion in Section 7.

2. Problem Formulation

In order to evaluate the effect of the radial electric field on the viscous liquid jets during centrifugal spinning, we assume that we have a cylindrical container which rotates with angular velocity Ω. The cylinder's axis is vertical and it rotates about its axis. There is a spinneret on a side of the rotating container with a nozzle of radius a from which the jet emanates. We denote with s_0 the distance between the axis of the rotating cylinder to the nozzle. The cartesian coordinate system x, y, z rotates with the container and the origin coincides with the nozzle of the spinneret. In this problem, we assume that the x and z axises are normal and tangential to the surface of nozzle respectively (see Figure 1). As we are interested in rapidly rotating jets, the effect of gravity is small, so we will neglect the gravity force in this problem. In many experiments with viscoelastic jets there is a copper collector where the nanofibers are collected, but we do not include it in our modelling.

In order to determine the position of the centreline of the curved liquid jet which moves in the plane $y = 0$, we use the functions $(x = X(s,t), z = Z(s,t))$, where s is the arc-length along the centreline of the jet, and t is the time. To describe the flow, we use the curvilinear coordinate system (s, n, ϕ), which are the tangential direction to the centreline of the liquid jet, and the radial and azimuthal coordinates respectively (see Wallwork (2002) and Decent et al. (2002)).

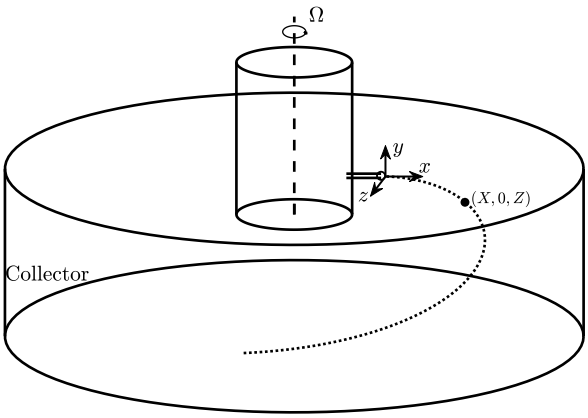

FIG. 1. Sketch of the flow. An electric potential is applied to the rotating container and the (copper) collector

The fluid governing equations can be written as

$$\nabla \cdot \mathbf{u} = 0,$$

$$\rho\left(\frac{\partial \mathbf{u}}{\partial t} + \mathbf{u}\cdot\nabla\mathbf{u}\right) = \nabla\cdot\tau - 2\,\omega\times\mathbf{u} - \omega\times(\omega\times\mathbf{r}),$$

$$\tau = \tau^{\mathbf{F}} + \tau^{\mathbf{E}},$$

$$\tau^{\mathbf{F}} = -p\mathbf{I} + \mu\nabla\mathbf{u} + (\nabla\mathbf{u})^{T}). \tag{2.1}$$

where $\mathbf{u}$ is the velocity in the form $\mathbf{u} = u\mathbf{e_s} + v\mathbf{e_n} + w\mathbf{e}_\phi$, ρ is the density of the fluid, $\mathbf{r}$ is the position vector of any particle, which is written as $\mathbf{r} = \int_0^s \mathbf{e_s}\,ds + n\,\mathbf{e_n}$, n is the radial distance, μ is the viscosity of the fluid, p is the fluid pressure, ω is the angular velocity of the container, $\tau^{\mathbf{F}}$ is the fluids stress tensor and $\tau^{\mathbf{E}}$ is the Maxwell stress tensor (see Saville (1997)) which contains the contributions of the electric field $\mathbf{E} = E_s\mathbf{e_s} + E_n\mathbf{e_n} + E_\phi\mathbf{e}_\phi$. The liquid is assumed to be a leaky dielectric of finite electrical conductivity K_1 and ε_1 is the fluids electrical permittivity. We also define ε_2 to be the dielectric constant/ permittivity of the air and assume the air to be a perfect dielectric. The dimensional equations of motion projected on our basis $(\mathbf{e_s}, \mathbf{e_n}, \mathbf{e}_\phi)$ are given in Appendix, see (8.1)-(8.4).

According to the Taylor-Melcher leaky dielectric theory (1969), the Gauss law in the bulk of the fluid for the electric field $\mathbf{E}$ and the motion of surface charge Q on the liquid surface are the following (see also Papageorgiou(2019) and Saville(1997))

$$\nabla\cdot(\varepsilon_1\mathbf{E}) = q, \tag{2.2}$$

$$\frac{\partial Q}{\partial t} + \mathbf{u}\cdot\nabla_s Q - Q\mathbf{n}\cdot(\mathbf{n}\cdot\nabla)u = [K_1\mathbf{E}\cdot\mathbf{n}]_2^1, \tag{2.3}$$

where q is free charge density in the fluid, ∇_s is the surface gradient operator and $\mathbf{n}$ the (outward) normal unit vector to the liquid jet. The position of the free surface is given by $n = R(s,\phi,t)$, so the outward unit normal vector to the free surface, $\mathbf{n}$, is

$$\mathbf{n} = \frac{1}{\Xi}\left(-\frac{\partial R}{\partial s}\frac{1}{h_s}\mathbf{e_s} + \mathbf{e_n} - \frac{\partial R}{\partial \phi}\frac{1}{R}\mathbf{e}_\phi\right),$$

where

$$\Xi = \left(1 + \frac{1}{h_s^2}\left(\frac{\partial R}{\partial s}\right)^2 + \frac{1}{R^2}\left(\frac{\partial R}{\partial \phi}\right)^2\right)^{\frac{1}{2}}.$$

The equations (2.2)-(2.3) can be projected in our basis and are given in full in dimensional form in Appendix (see (8.5)-(8.6)). From now on, we will consider here the non-dimensional form of all the equations. In particular, the equations (8.1)-(8.6) are non-dimensionalised using the transformation described in Uddin (2007). Consequently, the momentum equations and the continuity equation are similar to Uddin (2007) differing only in the terms of constitutive equations and electric field terms. We use the following scales

$$\begin{aligned}
&\bar{u} = \frac{u}{U},\ \bar{v} = \frac{v}{U},\ \bar{w} = \frac{w}{U},\ \bar{n} = \frac{n}{a},\ \varepsilon = \frac{a}{s_0},\ \bar{R} = \frac{R}{a},\ \bar{Q} = \frac{Q}{\varepsilon_2 E_0}\\
&\bar{\mathbf{E}} = \frac{\mathbf{E}}{E_0},\ \bar{s} = \frac{s}{s_0},\ \bar{t} = \frac{U}{s_0}t,\ \bar{p} = \frac{p}{\rho U^2},\ \bar{X} = \frac{X}{s_0},\ \bar{Z} = \frac{Z}{s_0},\ \bar{q} = \frac{s_0}{\varepsilon_1 E_0}q,
\end{aligned} \tag{2.4}$$

where U is the jet's exit speed in the rotating frame, s_0 is the distance from rotating axis of the cylindrical can containing the fluid to the nozzle of the spinneret, a is the radius of the nozzle, u,v,w are the tangential, radial and azimuthal velocity components, Q is the surface charge on the liquid surface, ε is the aspect ratio of the jet and E_0 is a characteristic field strength (note for example that Hohman et al. (2001) defines E_0 to be $\sqrt{\sigma/(\varepsilon_1-\varepsilon_2)a}$, where σ is the isotropic surface tension). After dropping the overbars, the governing dimensionless equations are the continuity equation

$$\varepsilon n\frac{\partial u}{\partial s} + h_s\left(v + n\frac{\partial v}{\partial n} + \frac{\partial w}{\partial \phi}\right) + \varepsilon n\left(v\cos\phi - w\sin\phi\right)\left(X_s Z_{ss} - Z_s X_{ss}\right) = 0, \tag{2.5}$$

and the momentum equations

$$
\begin{aligned}
&h_s\left(\varepsilon\frac{\partial u}{\partial t}+\varepsilon(v\cos\phi-w\sin\phi)(Z_{st}X_s-X_{st}Z_s)+v\frac{\partial u}{\partial n}+\frac{w}{n}\frac{\partial u}{\partial\phi}\right)\\
&+\varepsilon u\frac{\partial u}{\partial s}+\varepsilon u(v\cos\phi-w\sin\phi)(X_sZ_{ss}-Z_sX_{ss})=-\varepsilon\frac{\partial p}{\partial s}\\
&+\left(\frac{2\varepsilon}{Rb}(v\cos\phi-w\sin\phi)+\frac{\varepsilon}{Rb^2}((X+1)X_s+ZZ_s)\right)h_s\\
&+\frac{1}{\varepsilon Re}\left(\frac{-n\varepsilon^3\cos\phi(X_sZ_{sss}-Z_sX_{sss})}{h_s^2}\left(\frac{\partial u}{\partial s}+v\cos\phi(X_sZ_{ss}-Z_sX_{ss})\right.\right.\\
&\left.-w\sin\phi(X_sZ_{ss}-Z_sX_{ss})\right)+\frac{\varepsilon^2}{h_s}\left(-u(X_sZ_{ss}-Z_sX_{ss})^2\right.\\
&+\frac{\partial^2u}{\partial s^2}+2\frac{\partial v}{\partial s}\cos\phi(X_sZ_{ss}-Z_sX_{ss})+v\cos\phi(X_sZ_{sss}-Z_sX_{sss})-w\sin\phi(X_sZ_{sss}-Z_sX_{sss})\\
&\left.-2\frac{\partial w}{\partial s}\sin\phi(X_sZ_{ss}-Z_sX_{ss})\right)+(1+2\varepsilon n\cos\phi(X_sZ_{ss}-Z_sX_{ss}))\frac{1}{n}\frac{\partial u}{\partial n}\\
&\left.+h_s\frac{\partial^2u}{\partial n^2}+\frac{h_s}{n^2}\frac{\partial^2u}{\partial\phi^2}-\frac{\varepsilon}{n}\frac{\partial u}{\partial\phi}\sin\phi(X_sZ_{ss}-Z_sX_{ss})\right)+\varepsilon E_f(\beta+1)E_s\left[\frac{\partial E_s}{\partial s}\right.\\
&\left.+h_s\left(\frac{E_n}{n}+\frac{\partial E_n}{\partial n}\right)+\cos\phi(X_sZ_{ss}-Z_sX_{ss})E_n+\frac{h_s}{n}\frac{\partial E_\phi}{\partial\phi}-E_\phi\sin\phi(X_sZ_{ss}-Z_sX_{ss})\right].
\end{aligned}
\tag{2.6}
$$

$$h_s\left(\varepsilon\frac{\partial v}{\partial t}+\varepsilon u\cos\phi(X_{st}Z_s-Z_{st}X_s)+v\frac{\partial v}{\partial n}+\frac{w}{n}\frac{\partial v}{\partial\phi}-\frac{w^2}{n}\right)+\varepsilon u\frac{\partial v}{\partial s}-$$

$$\varepsilon u^2\cos\phi(X_sZ_{ss}-X_{ss}Z_s)=-\frac{\partial p}{\partial n}h_s-\frac{2\varepsilon}{Rb}h_s u\cos\phi+$$

$$\left(\frac{\varepsilon}{Rb^2}\cos\phi((X+1)Z_s-ZX_s+\varepsilon n\cos\phi)\right)h_s+$$

$$\frac{1}{Re}\left(\frac{-\varepsilon^2 n\cos\phi(X_sZ_{sss}-X_{sss}Z_s)}{h_s^2}\left(\frac{\partial v}{\partial s}-u\cos\phi(X_sZ_{ss}-X_{ss}Z_s)\right)+\right.$$

$$\frac{\varepsilon}{h_s}\left(-v\cos^2\phi\,(X_sZ_{ss}-X_{ss}Z_s)^2+\frac{\partial^2 v}{\partial s^2}-2\frac{\partial u}{\partial s}\cos\phi\,(X_sZ_{ss}-X_{ss}Z_s)-\right.$$

$$\left.u\cos\phi(X_sZsss-X_{sss}Z_s)+w\sin\phi\cos\phi(X_sZ_{ss}-X_{ss}Z_s)^2\right)+$$

$$(1+2\varepsilon n\cos\phi(X_sZ_{ss}-X_{ss}Z_s))\frac{1}{\varepsilon n}\frac{\partial v}{\partial n}+\frac{h_s}{n}\frac{\partial^2 v}{\partial n^2}-\frac{1}{n}(\frac{\partial v}{\partial\phi}-w)\sin\phi(X_sZ_{ss}-X_{ss}Z_s)+$$

$$\left.\frac{h_s}{\varepsilon n^2}(\frac{\partial^2 v}{\partial\phi^2}-v-2\frac{\partial w}{\partial\phi})\right)+\varepsilon E_f(\beta+1)E_n\left[\frac{\partial E_s}{\partial s}+h_s\left(\frac{E_n}{n}+\frac{\partial E_n}{\partial n}\right)+\cos\phi(X_sZ_{ss}-Z_sX_{ss})E_n\right.$$

$$\left.+\frac{h_s}{n}\frac{\partial E_\phi}{\partial\phi}-E_\phi\sin\phi(X_sZ_{ss}-Z_sX_{ss})\right], \tag{2.7}$$

$$h_s\left(\varepsilon\frac{\partial w}{\partial t}+\varepsilon u\sin\phi(Z_{st}X_s-X_{st}Z_s)+v\frac{\partial w}{\partial n}+\frac{w}{n}\frac{\partial w}{\partial\phi}-\frac{vw}{n}\right)+\varepsilon u\frac{\partial w}{\partial s}+$$

$$\varepsilon u^2\sin\phi(X_sZ_{ss}-X_{ss}Z_s)=\left(-\frac{1}{n}\frac{\partial p}{\partial\phi}h_s+\frac{2\varepsilon}{Rb}u\sin\phi+\right.$$

$$\left.\frac{\varepsilon}{Rb^2}\sin\phi(ZX_s-(X+1)Z_s-n\cos\phi)\right)h_s+$$

$$\frac{1}{Re}\left(\frac{-\varepsilon^2 n\cos\phi(X_sZ_{sss}-X_{sss}Z_s)}{h_s^2}\left(\frac{\partial w}{\partial s}+u\sin\phi(X_sZ_{ss}-X_{ss}Z_s)\right)+\right.$$

$$\frac{\varepsilon}{h_s}\left(-w\sin^2\phi\,(X_sZ_{ss}-X_{ss}Z_s)^2+\frac{\partial^2 w}{\partial s^2}+2\frac{\partial u}{\partial s}\sin\phi\,(X_sZ_{ss}-X_{ss}Z_s)+\right.$$

$$\left.u\sin\phi(X_sZ_{sss}-X_{sss}Z_s)+v\sin\phi\cos\phi(X_sZ_{ss}-X_{ss}Z_s)^2\right)+$$

$$(1+2\varepsilon n\cos\phi(X_sZ_{ss}-X_{ss}Z_s))\frac{1}{\varepsilon n}\frac{\partial w}{\partial n}+\frac{h_s}{\varepsilon}\frac{\partial^2 w}{\partial n^2}-\frac{1}{\varepsilon}(\frac{\partial w}{\partial\phi}+v)\sin\phi(X_sZ_{ss}-X_{ss}Z_s)+$$

$$\left.\frac{h_s}{\varepsilon n^2}(\frac{\partial^2 w}{\partial\phi^2}-w+2\frac{\partial v}{\partial\phi})\right)+\varepsilon E_f(\beta+1)E_\phi\left[\frac{\partial E_s}{\partial s}+h_s\left(\frac{E_n}{n}+\frac{\partial E_n}{\partial n}\right)\right.$$

$$\left.+\cos\phi(X_sZ_{ss}-Z_sX_{ss})E_n+\frac{h_s}{n}\frac{\partial E_\phi}{\partial\phi}-E_\phi\sin\phi(X_sZ_{ss}-Z_sX_{ss})\right], \tag{2.8}$$

where $h_s=1+\varepsilon n\cos\phi(X_sZ_{ss}-X_{ss}Z_s)$, and X_s, X_{ss}, Z_s, Z_{ss} denote partial derivatives with respect to s.

The equations concerning the surface charge and the electric field (8.5) and (8.6) in dimensionless form become

$$\varepsilon n\frac{\partial E_s}{\partial s}+h_s\left(\frac{\partial(nE_n)}{\partial n}+\frac{\partial E_\phi}{\partial\phi}\right)+\varepsilon n\left(E_n\cos\phi-E_\phi\sin\phi\right)(X_sZ_{ss}-Z_sX_{ss})=\varepsilon nh_s q, \tag{2.9}$$

$$\frac{\partial Q}{\partial t}+u\frac{1}{h_s}\cdot\frac{\partial Q}{\partial s}\left[1-\frac{1}{\Xi^2}\left(\varepsilon\frac{\partial R}{\partial s}\cdot\frac{1}{h_s}\right)^2\right]+\frac{v}{\varepsilon}\frac{\partial Q}{\partial n}(1-\frac{1}{\Xi^2})+\frac{w}{\varepsilon}\cdot\frac{1}{n}\cdot\frac{\partial Q}{\partial\phi}\left[1-\frac{1}{\Xi^2}\left(\frac{\partial R}{\partial\phi}\cdot\frac{1}{R}\right)^2\right]$$
$$-\frac{Q}{\Xi^2}\left\{\left(-\varepsilon\frac{\partial R}{\partial s}\right)\cdot\frac{1}{h_s^2}\left[\left(-\varepsilon\frac{\partial R}{\partial s}\right)\cdot\frac{1}{h_s^2}\left(\frac{\partial u}{\partial s}+\left(X_sZ_{ss}-X_{ss}Z_s\right)\left(u\cos\phi-u\sin\phi\right)\right)\right.\right.$$
$$\left.+\frac{1}{\varepsilon}\frac{\partial u}{\partial n}+\left(-\frac{\partial R}{\partial\phi}\right)\cdot\frac{1}{R}\cdot\frac{1}{\varepsilon n}\cdot\frac{\partial u}{\partial\phi}\right]+\left(-\varepsilon\frac{\partial R}{\partial s}\right)\cdot\frac{1}{h_s^2}\left(\frac{\partial v}{\partial s}-\left(X_sZ_{ss}-X_{ss}Z_s\right)u\cos\phi+\frac{\partial v}{\varepsilon\partial n}\right)$$
$$+\left(-\frac{\partial R}{\partial\phi}\right)\cdot\frac{1}{R}\cdot\frac{1}{\varepsilon n}\left(\frac{\partial v}{\partial\phi}-w\right)+\left(-\frac{\partial R}{\partial\phi}\right)\cdot\frac{1}{R}\cdot\left[\left(-\varepsilon\frac{\partial R}{\partial s}\right)\cdot\frac{1}{h_s^2}\left(\frac{\partial w}{\partial s}+\left(X_sZ_{ss}-X_{ss}Z_s\right)\right.\right.$$
$$\left.\left.\left.u\sin\phi+\frac{\partial w}{\varepsilon\partial n}\right)+\left(-\frac{\partial R}{\partial\phi}\right)\cdot\frac{1}{R}\cdot\frac{1}{\varepsilon n}\left(\frac{\partial w}{\partial\phi}+v\right)\right]\right\}=\frac{\bar{K}}{\Xi}\left(-\frac{\partial R}{\partial s}E_s+\frac{E_n}{\varepsilon}-\frac{1}{\varepsilon}\frac{\partial R}{\partial\phi}\frac{E_\phi}{R}\right). \quad (2.10)$$

The governing equations for the fluid are similar to the ones found in Părău *et al*. (2007), but they have extra terms related to the electric field. The equations (2.9) and (2.10) are the new ones related to the electric field and surface charge. However, as mentioned in Papageorgiou (2019), for incompressible fluid with constant ε_1 and K_1, all the electric charge will be depleted from bulk of the fluid and will move to the jet surface, so we will assume $q=0$ from now on. Then the equation (2.9) also implies that the explicit electric terms from the equations (2.6)-(2.8) will disappear.

The dimensionless parameters in the problem are: the Rossby number $Rb=\frac{U}{s_0\Omega}$, the Weber number $We=\frac{\rho U^2 a}{\sigma}$, the Reynolds number $Re=\frac{\rho U s_0}{\mu}$, the dielectric constant ratio $\beta=\frac{\varepsilon_1}{\varepsilon_2}-1$, the electric force parameter $E_f=\frac{\varepsilon_2 E_0^2}{\rho U^2}$ and the dimensionless conductivity of the fluid $\bar{K}=\frac{K_1 a}{U\varepsilon_2}$. We also find it useful to introduce $\tilde{E_f}=\frac{\varepsilon_2 E_0^2 s_0}{\rho U^2 a}=\frac{E_f}{\varepsilon}$.

3. Boundary conditions

The normal stress condition at the free surface is

$$n^T\cdot\tau\cdot\mathbf{n}\Big|_{\mathbf{2}}^{\mathbf{1}}=\sigma\kappa,$$

where $\tau=\tau^{\mathbf{F}}+\tau^{\mathbf{E}}$ is the total stress tensor, σ is the isotropic surface tension and κ is the curvature of the free surface. The components of the stress tensor $\tau^{\mathbf{F}}$ in the curvilinear coordinate system used in this problem are given in Appendix. After some algebra, it can be shown that the normal stress condition becomes in non-dimensional form

$$
\begin{aligned}
&p-\frac{2}{Re}\frac{1}{\Xi^2}\left(\varepsilon^2\left(\frac{\partial R}{\partial s}\right)^2\frac{1}{h_s^3}\left(\frac{\partial u}{\partial s}+(v\,cos\phi-\sin\phi)(X_sZ_{ss}-Z_sX_{ss})\right)\right.\\
&+\frac{1}{\varepsilon}\frac{\partial v}{\partial n}+\frac{1}{\varepsilon R^3}\left(\frac{\partial R}{\partial \phi}\right)^2\left(\frac{\partial w}{\partial \phi}+v\right)-\frac{\varepsilon}{h_s}\frac{\partial R}{\partial s}\left(\frac{1}{h_s}\frac{\partial v}{\partial s}\right.\\
&\left.+\frac{1}{\varepsilon}\frac{\partial u}{\partial n}-\frac{u}{h_s}cos\phi(X_sZ_{ss}-Z_sX_{ss})\right)+\frac{\varepsilon}{Rh_s}\frac{\partial R}{\partial s}\frac{\partial R}{\partial \phi}\left(\frac{1}{\varepsilon R}\frac{\partial u}{\partial \phi}\right.\\
&\left.\left.+\frac{u}{h_s}\sin\phi(X_sZ_{ss}-Z_sX_{ss})+\frac{1}{h_s}\frac{\partial u}{\partial s}\right)-\frac{1}{\varepsilon R}\frac{\partial R}{\partial \phi}\left(R\frac{\partial w}{\partial n}-\frac{w}{R}+\frac{1}{R}\frac{\partial v}{\partial \phi}\right)\right)\\
&+\frac{E_f}{2}\left\{Q^2+2(\beta+1)Q\left(\frac{1}{\Xi}\left(-\frac{\partial R}{\partial s}\cdot\frac{\varepsilon}{h_s}.E_s+E_n-\frac{\partial R}{\partial \phi}\cdot\frac{1}{R}.E_\phi\right)\right)\right.\\
&+\beta(\beta+1)\left(\frac{1}{\Xi}\left(-\frac{\partial R}{\partial s}\cdot\frac{\varepsilon}{h_s}.E_s+E_n-\frac{\partial R}{\partial \phi}\cdot\frac{1}{R}.E_\phi\right)\right)^2\\
&\left.+\beta\frac{1}{\left(1+\left(\frac{\partial R}{\partial s}\frac{\varepsilon}{h_s}\right)^2\right)}\left(E_s+\frac{\partial R}{\partial s}\frac{\varepsilon}{h_s}E_n\right)^2+\beta\frac{1}{\left(1+\left(\frac{\partial R}{\partial \phi}\frac{1}{R}\right)^2\right)}\left(\frac{\partial R}{\partial \phi}\frac{1}{R}E_n+E_\phi\right)^2\right\}=\frac{\kappa}{We},
\end{aligned}
\tag{3.1}
$$

where

$$
\kappa=\frac{1}{h_s}\left(-\varepsilon^2\frac{\partial}{\partial s}\left(\frac{1}{\Xi\,h_s}\frac{\partial R}{\partial s}\right)+\frac{1}{n}\frac{\partial}{\partial n}\left(\frac{nh_s}{\Xi}\right)-\frac{\partial}{\partial \phi}\left(\frac{h_s}{\Xi\,n^2}\frac{\partial R}{\partial \phi}\right)\right).
$$

$$
\Xi=\left(1+\frac{\varepsilon^2}{h_s^2}\left(\frac{\partial R}{\partial s}\right)^2+\frac{1}{R^2}\left(\frac{\partial R}{\partial \phi}\right)^2\right)^{\frac{1}{2}}.
$$

The tangential stress conditions at the free surface are

$$
\mathbf{t_i}^T\cdot\boldsymbol{\tau}^{\mathbf{F}}\cdot\mathbf{n}\Big|_2^1=Q\mathbf{E}\cdot\mathbf{t_i},
$$

where $\mathbf{t_i}$ are the tangent vectors $i=1,2$.

The first tangential stress condition is in non-dimensional form

$$\begin{aligned}
&\left(1-\varepsilon^2\left(\frac{\partial R}{\partial s}\right)^2\frac{1}{h_s^2}\right)\frac{1}{\Xi h_s}\left\{\varepsilon\frac{\partial v}{\partial s}+h_s\frac{\partial u}{\partial n}-\varepsilon u\cos\phi(X_sZ_{ss}-X_{ss}Z_s)\right\}\\
&+\frac{2}{\Xi h_s}\varepsilon\frac{\partial R}{\partial s}\left\{\frac{\partial v}{\partial n}-\varepsilon\frac{\partial u}{\partial s}\frac{1}{h_s}-\frac{\varepsilon}{h_s}(v\cos\phi-w\sin\phi)(X_sZ_{ss}-X_{ss}Z_s)\right\}\\
&-\frac{1}{\Xi}\frac{\partial R}{\partial\phi}\left\{\frac{\partial u}{\partial\phi}+\frac{\varepsilon}{h_s}u\sin\phi(X_sZ_{ss}-X_{ss}Z_s)+\frac{\varepsilon}{h_s}\frac{\partial w}{\partial s}+\frac{\varepsilon}{h_s}\left(\frac{\partial w}{\partial n}-\frac{w}{R}+\frac{1}{R}\frac{\partial v}{\partial\phi}\right)\right\}\\
&=\varepsilon^2\tilde{E}_f\cdot Re\cdot Q\left\{E_s+\frac{\varepsilon}{h_s}\frac{\partial R}{\partial s}E_n\right\},
\end{aligned}\tag{3.2}$$

and the second tangential stress condition is

$$\begin{aligned}
&\left(1-\left(\frac{\partial R}{\partial\phi}\right)^2\frac{1}{R^2}\right)\frac{1}{\Xi}\left(\frac{\partial w}{\partial n}-\frac{w}{R}+\frac{1}{R}\frac{\partial v}{\partial\phi}\right)+\frac{2}{\Xi R}\frac{\partial R}{\partial\phi}\left(\frac{\partial v}{\partial n}-\frac{1}{R}\left(\frac{\partial w}{\partial\phi}+v\right)\right)\\
&-\frac{1}{\Xi}\frac{\partial R}{\partial s}\frac{\varepsilon}{h_s}\left\{\frac{1}{R}\frac{\partial u}{\partial\phi}+\frac{\varepsilon}{h_s}u\sin\phi(X_sZ_{ss}-X_{ss}Z_s)+\frac{\varepsilon}{h_s}\frac{\partial w}{\partial s}\right.\\
&\left.+\frac{\partial R}{\partial\phi}\frac{1}{R}\left(\frac{\varepsilon}{h_s}\frac{\partial v}{\partial s}+\frac{\partial u}{\partial n}-\frac{\varepsilon}{h_s}u\cos\phi(X_sZ_{ss}-X_{ss}Z_s)\right)\right\}\\
&=\varepsilon^2\tilde{E}_f\cdot Re\cdot Q\left\{\frac{1}{R}\frac{\partial R}{\partial\phi}E_n+E_\phi\right\}.
\end{aligned}\tag{3.3}$$

Another equation needed is the arc-length condition $X_s^2+Z_s^2=1$.

The kinematic condition at the surface of the jet is

$$\begin{aligned}
&h_s\left(\varepsilon\frac{\partial R}{\partial t}+\cos\phi(X_tZ_s-X_sZ_t)+\frac{1}{R}\frac{\partial R}{\partial\phi}\sin\phi(X_tZ_s-X_sZ_t)-v+\frac{\partial R}{\partial\phi}\frac{w}{R}\right)\\
&+\varepsilon u\frac{\partial R}{\partial s}-\varepsilon\frac{\partial R}{\partial s}(X_tX_s+Z_tZ_s+\varepsilon R\cos\phi(X_sZ_{ss}-Z_sX_{ss}))=0.
\end{aligned}\tag{3.4}$$

4. Asymptotic analysis and one-dimensional equations

Using asymptotic analysis we will derive the one-dimensional model equations for the curved liquid jet. We assume the jet is slender $\varepsilon\ll 1$, and using the radial expansion method (see Eggers (1997) and Hohman *et al*. (1984) with a different notation), we expand u,v,w and p in Taylor's series on εn, and X,Z,R,Q,E_s,E_n in an asymptotic series in ε. Here, the axial velocity component at the leading order is supposed to be independent of ϕ, as we look for slender liquid jets with circular cross section at leading order and where the velocity is parallel to the centreline at leading order. We also assume that

the centreline is steady which was justified in Părău et al. (2007). Thus, we have

$$
\begin{aligned}
&(u,v,w)(s,n,\phi,t) = (u_0,0,0)(s,t) + (\varepsilon n)(u_1,v_1,w_1)(s,\phi,t) + ...\\
&p(s,n,\phi,t) = p_0(s,\phi,t) + (\varepsilon n)p_1(s,\phi,t) + ...\\
&(R,Q)(s,n,\phi,t) = (R_0,Q_0)(s,t) + (\varepsilon)(R_1,Q_1)(s,\phi,t) + ...\\
&(X,Z)(s,n,\phi,t) = (X_0,Z_0)(s) + (\varepsilon)(X_1,Z_1)(s) + ...\\
&(E_s,E_n,E_\phi)(s,n,\phi,t) = (E_0,0,0)(s,t) + (\varepsilon n)(E_{s1},E_{n1},E_{\phi 1})(s,\phi,t) + ...
\end{aligned}
$$

For simplicity of notation, we drop the subscript for the centreline quantities and denote X_0, Z_0 as X, Z. From the continuity equation, we obtain

$$O(\varepsilon n): \quad u_{0s} + 2v_1 + w_{1\phi} = 0, \tag{4.1}$$

$$O(\varepsilon n)^2: \quad u_{1s} + 3v_2 + w_{2\phi} + 3v_1 + \left(w_{1\phi}\cos\phi - w_1\sin\phi\right)(X_sZ_{ss} - X_{ss}Z_s) = 0. \tag{4.2}$$

By solving the second tangential stress condition, we obtain

$$O(\varepsilon): \quad R_0^3 v_{1\phi} = 0, \tag{4.3}$$

$$O(\varepsilon)^2: \quad 3R_0^2R_1v_{1\phi} + R_0^4(w_2 + v_{2\phi}) - 2R_0^2R_{1\phi}w_{1\phi} = 0. \tag{4.4}$$

It can be observed that $v_{1\phi} = 0$, and by differentiating (4.1), we obtain $w_{1\phi\phi} = 0$. Because w_1 is periodic in ϕ we must have $w_1 = w_1(s,t)$. That leads to $v_1 = -\frac{u_{0s}}{2}$ and from (4.4) we obtain

$$w_2 + v_{2\phi} = 0. \tag{4.5}$$

From the electric equation (2.9), we get at leading order

$$E_{1n} = -\frac{1}{2}\frac{\partial E_0}{\partial s}. \tag{4.6}$$

We now substitute this equation (4.6) into (2.10), and after some algebra using the kinematic condition (3.4) at leading order ε, the surface charge density equation at leading order becomes

$$\frac{\partial}{\partial t}\left(2R_0Q_0\right) + \frac{\partial}{\partial s}\left(2R_0u_0Q_0 + R_0^2\bar{K}E_0\right) = 0, \tag{4.7}$$

Using the first tangential stress condition, it can be obtained that

$$O(\varepsilon): \quad u_1 = u_0\cos\phi(X_sZ_{ss} - X_{ss}Z_s), \tag{4.8}$$

$$O(\varepsilon)^2: \quad u_2 = \frac{3}{2}u_{0s}\frac{R_{0s}}{R_0} + \frac{u_{0ss}}{4} + \frac{1}{2R_0}Re\,\tilde{E}_f Q_0E_0. \tag{4.9}$$

By differentiating (4.5) with respect to ϕ we have

$$w_{2\phi} = -v_{2\phi\phi}, \tag{4.10}$$

hence

$$v_{2\phi\phi} - 3v_2 = u_{1s} + (3v_1\cos\phi - w_1\sin\phi)(X_sZ_{ss} - X_{ss}Z_s), \tag{4.11}$$

so when the expression for u_1 and v_1 are used, we obtain

$$v_{2\phi\phi} - 3v_2 = \left(u_0(X_sZ_{sss} - X_{sss}Z_s) - \frac{u_{0s}}{2}(X_sZ_{ss} - X_{ss}Z_s)\right)\cos\phi - w_1\sin\phi(X_sZ_{ss} - X_{ss}Z_s). \quad (4.12)$$

But v_2 and w_2 are periodic solutions, hence

$$v_2 = \frac{1}{4}\left(\frac{u_{0s}}{2}(X_sZ_{ss} - X_{ss}Z_s) - u_0(X_sZ_{sss} - X_{sss}Z_s)\right)\cos\phi + \frac{w_1}{4}\sin\phi(X_sZ_{ss} - X_{ss}Z_s), \quad (4.13)$$

and

$$w_2 = \frac{1}{4}\left(\frac{u_{0s}}{2}(X_sZ_{ss} - X_{ss}Z_s) - u_0(X_sZ_{sss} - X_{sss}Z_s)\right)\sin\phi + \frac{w_1}{4}\cos\phi(X_sZ_{ss} - X_{ss}Z_s). \quad (4.14)$$

Based on the momentum equation in the radial direction, we get at leading order $p_{0n} = 0$ and at order ε

$$\begin{aligned} p_1 = &\left(u_0^2(X_sZ_{ss} - X_{ss}Z_s) - \tfrac{2}{Rb}u_0 + \tfrac{(X+1)Z_s - ZX_s}{Rb^2}\right)\cos\phi \\ &-\tfrac{1}{Re}\left(\tfrac{5}{2}u_{0s}(X_sZ_{ss} - X_{ss}Z_s) + u_{0s}(X_sZ_{sss} - X_{sss}Z_s)\right)\cos\phi + \tfrac{1}{Re}w_1\sin\phi(X_sZ_{ss} - X_{ss}Z_s). \end{aligned} \quad (4.15)$$

From the momentum equation in the azimuthal direction, we have at leading order, $p_{0\phi} = 0$. At the next order in ε, we obtain the equation given above. At the leading order, the normal stress condition is given by

$$p_0 = -\frac{u_{0s}}{Re} + \frac{1}{R_0We} - E_f\frac{Q_0^2}{2} - E_f\frac{\beta}{2}E_0^2, \quad (4.16)$$

and we also have at order ε

$$p_1 = \frac{1}{R_0We}\left(-\frac{R_{1\phi\phi} + R_1}{R_0^2} + \cos\phi(X_sZ_{ss} - X_{ss}Z_s)\right) + \frac{4v_2}{Re}. \quad (4.17)$$

By substituting the expression for v_2, we obtain

$$\begin{aligned} p_1 = &\tfrac{1}{R_0We}\left(-\tfrac{R_{1\phi\phi}+R_1}{R_0^2} + \cos\phi(X_sZ_{ss} - X_{ss}Z_s)\right) + \\ &\tfrac{1}{Re}\left(\tfrac{u_{0s}}{2}(X_sZ_{ss} - X_{ss}Z_s) - u_0(X_sZ_{sss} - X_{sss}Z_s)\right)\cos\phi + \tfrac{w_1}{Re}\sin\phi(X_sZ_{ss} - X_{ss}Z_s). \end{aligned} \quad (4.18)$$

If we substitute p_1 from (4.15) in the previous equation, we obtain

$$(X_sZ_{ss} - X_{ss}Z_s)\left(u_0^2 - \frac{3}{Re}u_{0s} - \frac{1}{WeR_0}\right) - \frac{2}{Rb}u_0 + \frac{(X+1)Z_s - ZX_s}{Rb^2} = 0. \quad (4.19)$$

The Navier-Stokes equation in the axial direction at order ε is

$$u_{0t} + u_0u_{0s} = -p_{0s} + \frac{(X+1)X_s + ZZ_s}{Rb^2} + \frac{1}{Re}\left(u_{0ss} + 4u_2 + u_{2\phi\phi}\right). \quad (4.20)$$

After substituting the expressions for u_2 and p_0, the previous equation becomes

$$\begin{aligned} u_{0t} + u_0u_{0s} = &-\frac{1}{We}\left(\frac{1}{R_0}\right)_s + \frac{(X+1)X_s + ZZ_s}{Rb^2} \\ &+\frac{3}{Re}\left(u_{0ss} + 2u_{0s}\frac{R_{0s}}{R}\right) + \tilde{E_f}\left(\frac{2}{R_0}Q_0E_0\right) + E_f\left(Q_0Q_{0s} + \beta E_0E_{0s}\right). \end{aligned} \quad (4.21)$$

From the kinematic condition at order ε, we obtain

$$R_{0t} + \frac{u_{0s}}{2} R_0 + u_0 R_{0s} = 0. \tag{4.22}$$

The last equation to close the systems is the arc-length condition

$$X_s^2 + Z_s^2 = 1. \tag{4.23}$$

5. Steady State Solutions

By calculating steady state solutions and using the initial conditions at $s = 0$ $R_0(0) = 1$ and $u_0(0) = 1$, we obtain $R_0^2 u_0 = 1$ from the steady form of (4.22). Equations (4.21), (4.19) and (4.7) in steady form are

$$\begin{aligned} u_0 u_{0s} = &-\frac{1}{2We}\frac{u_{0s}}{\sqrt{u}} + \frac{(X+1)X_s + ZZ_s}{Rb^2} \\ &+ \frac{3}{Re}\left(u_{0ss} - \frac{u_{0s}^2}{u_0}\right) + \tilde{E_f}\left(2Q_0 E_0 \sqrt{u_0}\right) + E_f\left(Q_0 Q_{0s} + \beta E_0 E_{0s}\right), \end{aligned} \tag{5.1}$$

$$(X_s Z_{ss} - X_{ss} Z_s)\left(u_0^2 - \frac{3}{Re}u_{0s} - \frac{\sqrt{u}_0}{We}\right) - \frac{2}{Rb}u_0 + \frac{(X+1)Z_s - ZX_s}{Rb^2} = 0, \tag{5.2}$$

$$\frac{2Q_0\sqrt{u_0}}{\bar{K}} + \frac{E_0}{u_0} = 1. \tag{5.3}$$

It can be observed that when $Q_0 = E_0 = 0$, these equations reduce to the equations found in Părău et al. (2007). We consider in this problem an external electric radial field $\mathbf{E}_\infty$.

Hence, at a given point s on the jet centreline, by writing the electric radial field in polar coordinates we obtain that the external electric field is

$$\mathbf{E}_\infty = E_\infty \frac{(X+1)\mathbf{i} + Z\mathbf{k}}{(X+1)^2 + Z^2},$$

where E_∞ is a dimensionless parameter which describe the strength of the external electric field (see also Hashemi et al. (2018) eq. 14). We can write a boundary integral equation for the electric field on the surface of the jet as in Stone et al. (1999) eq. (2.4), for example. After projecting it on the tangential direction we obtain at leading order an expression for $E_0(s)$ in the form:

$$E_0 - \ln\left(\frac{1}{\chi}\right)\left[\frac{\beta}{2}\left(\frac{E_0}{u_0}\right)_{ss} - \sqrt{\beta}\left(\frac{Q_0}{\sqrt{u_0}}\right)_s\right] = E_\infty \frac{(X+1)X_s + ZZ_s}{(X+1)^2 + Z^2}, \tag{5.4}$$

where χ is the aspect ratio of the jet, which can be taken here to be $\chi^{-1} = \varepsilon = a/s_0$ (see Hohman et al. (2001a), Yarin et al. (2001) for more details on the derivation for the case of a uniform electric field applied to axisymmetric jets and extensions to curved liquid jets). Feng (2002) has solved the steady equations for an axismmetric liquid jet with an external uniform electric field instead of a radial one by using an equation similar with (5.4). They found that various conditions at the nozzle $R(0), E(0)$

etc. and at infinity have a strong influence on the results and some ad-hoc conditions were needed to solve the system and to match the solutions to experimental results (see also Hohman et al. (2001a)). Other authors (e.g. Spivak and Dzenis (1998)) have neglected the second term from the left hand side of (5.4) for their work on axisymmetric jets under an uniform electric field. In this paper we follow their approach, for simplicity, and we chose to neglect the second term on the left hand side (5.4). Hence we will consider

$$E_0(s) = E_\infty \frac{(1+X)X_s + ZZ_s}{(1+X)^2 + Z^2}. \tag{5.5}$$

Thus, the equation (5.5) assumes that the electric field $E_0(s)$ is directly influenced just by the imposed external radial electric field and in this paper we take a simplified approach by neglecting other terms which appear due to other electrical interactions. The analysis of the full equation (5.4) and a comprehensive study of the potential errors introduced by our simplification will be investigated in a future work.

The system of non-linear differential equations (4.23), (5.1)-(5.3) and (5.5) with the initial conditions $X = Z = Q_0 = E_{0s} = Z_s = 0$, and $u_0 = E_0 = X_s = 1$ at $s = 0$ can be solved using a finite difference scheme. This method based on Newton's method to solve nonlinear equations was applied by Părău et al. (2007) to solve the above equations in the absence of any electric field. They also compared their results with the Runge-Kutta method for the inviscid one and the results appeared identical for the steady centreline and radius of the jet.

It is worth discussing the range of parameters used in experiments, even though they are performed with viscoelastic fluids while our model here is for a viscous fluid. For example, Liao et al. (2011) has performed experiments to produce polylactic acid (PLA) nanofibers while Liao et al. (2011a) and Chang et al. (2014) has produced polyacrylonitrile (PAN) nanofibers. The viscosity μ of the solutions used in their experiments was in the range $19cP$ to $300cP$, the surface tension σ was between $25mN/m$ and $40mN/m$, the density ρ was varying between $0.97g/mL$ and $1.56g/mL$. The flow rate of the solution poured on the rotating container was between $0.25mL/h$ to $1mL/h$ and the exit velocity U was estimated to be around $100mL/hcm^2$. The voltage was chosen to be between $10kV$ and $30kV$, the conductivity K_1 of the solution was between $0.1\mu S$ and $1\mu S$. The container containing the solutions has a diameter of $6cm$ which, together with the attached a syringe/spinneret, gives an estimation of s_0 between $5cm$ and $8cm$. The cylinder was rotating at $1800rpm$ which gives $\Omega = 188rads/s$. The collector had a diameter of $40cm$ or $50cm$. The nanofibers obtained have diameters between $200nm$ and $5000nm$. The initial radius a of the jet at the spinneret was between $0.1mm$ and $2.5mm$

The non-dimensional quantities given for the experiments are estimated to be in the following ranges: $\varepsilon \approx 0.002..0.05$, $Re \approx 0.2..50$, $We \approx 0.15..30$, $Rb \approx 10^{-3}..10^{0}$. We also estimate β to be in the range 1..3. The other parameters E_f, $\bar{K}$ can also be, in principle, calculated.

The trajectory of viscous curved jets are displayed in Figs. 2, 3 and 4 for different values of E_f, E_∞ and Rb respectively. From these figures it can be noted that when we decrease these dimensionless numbers the jet coils more, which means that the rotation rate and the electric field have affected the trajectory of the jet. This was also observed in experiments with non-Newtonian fluids (see Liao et al. (2011a)) where they noted that the curvature radius increases with the external electric field. We also plotted the radius along the the jet for three values of E_∞ and E_f, and we observe that when we increase E_∞ and E_f, the jet radius reduces (see Figs. 5 and 6)). Liao et al. (2011a) have also noted that the diameter of nanofibers produced decreases when the electric field is increased in their experiments, which means that the jet radius is decreasing as s increases. On Fig. 7, it can be seen that the surface charge increases more for high rotation rates along the jet, while the electric field decreases (see Fig.8).

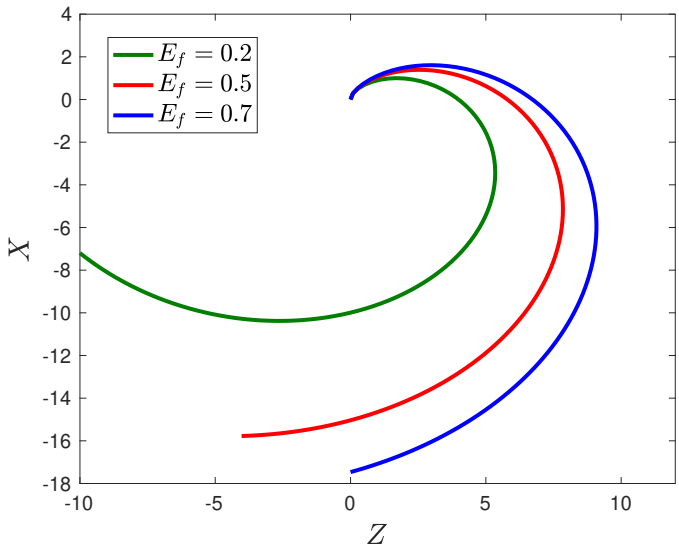

FIG. 2. Jet trajectory in the xz plane for different values of electric force parameter E_f. The other parameters are $We = 10$, $\bar{E_f} = 2$, 5 and 7, $Rb = 1$, $\bar{K} = 10$, $E_\infty = 5$ and $\beta = 40$.

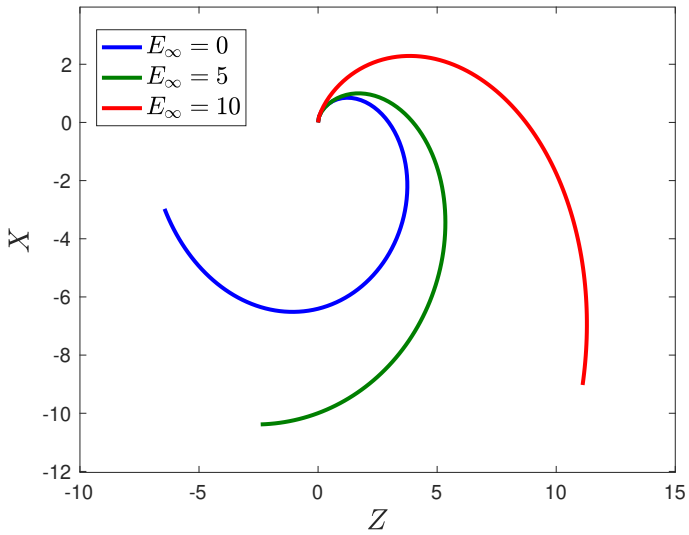

FIG. 3. Jet trajectory in the xz plane for different values of the external electric field E_∞. The other parameters are $We = 10$, $\bar{E_f} = 2$, $Rb = 1$, $\bar{K} = 10$, $E_f = 0.2$ and $\beta = 40$.

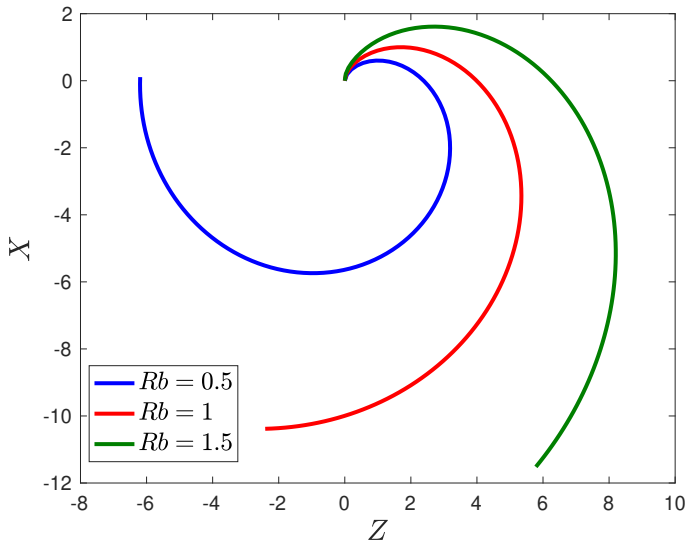

FIG. 4. Jet trajectory in the xz plane for different values of the Rossby number Rb. The other parameters are $We = 10$, $E_f = 0.2$, $\bar{K} = 0.1$, $\bar{E_f} = 2$, $E_\infty = 5$ and $\beta = 40$.

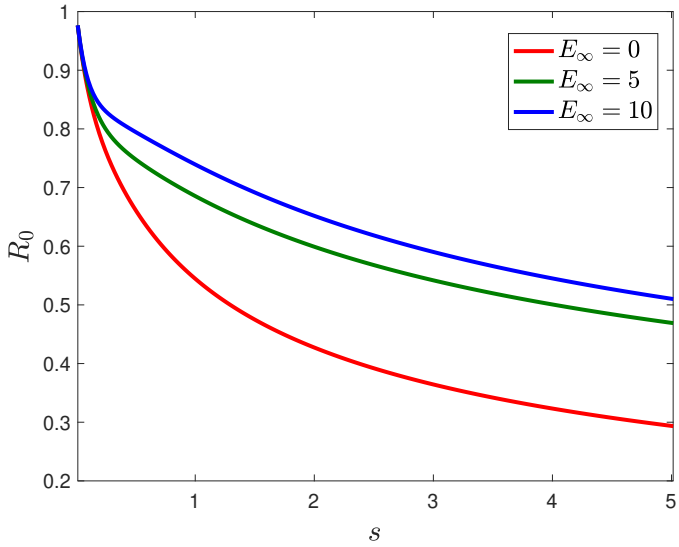

FIG. 5. Jet radius versus arc length for different values of the external electric field E_∞. The other parameters are $We = 10$, $Rb = 1$, $\bar{E_f} = 2$, $\bar{K} = 0.1$, $E_f = 0.2$ and $\beta = 40$.

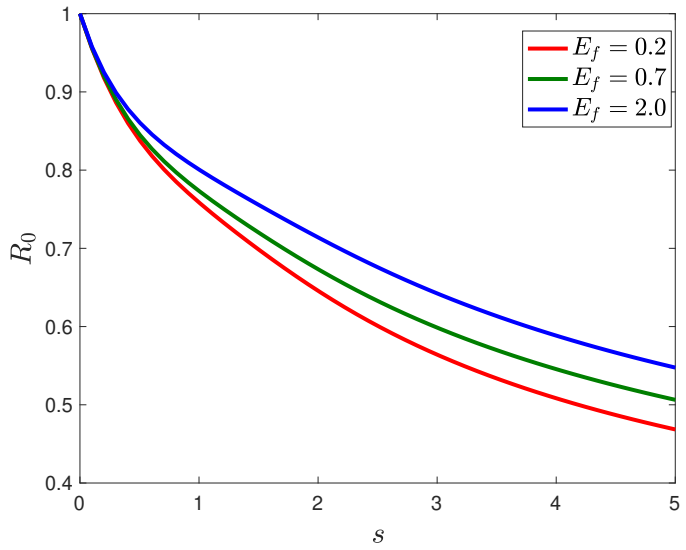

FIG. 6. Jet radius versus arc length for different values of electric force parameter E_f. The other parameters are $We = 10$, $Rb = 1$, $\bar{E_f} = 2$, 7 and 20, $\bar{K} = 0.1$, $E_\infty = 2$ and $\beta = 40$.

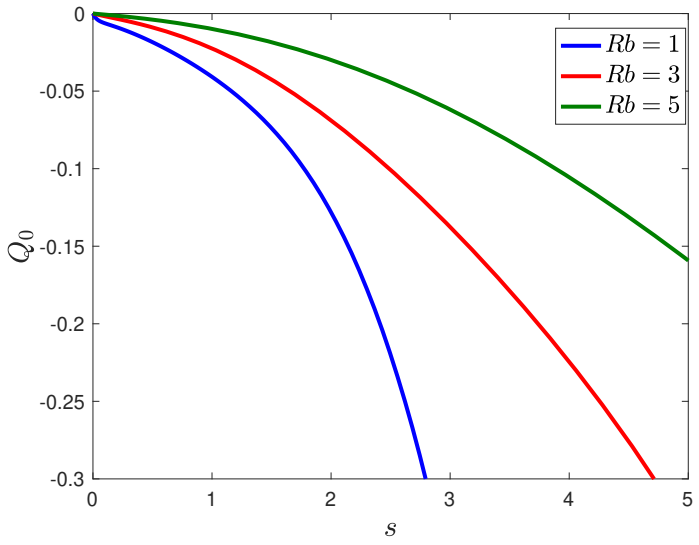

FIG. 7. Surface charge versus arc length for different values of the Rossby number Rb. The other parameters are $We = 10$, $\bar{K} = 0.1$, $E_f = 200$, $\beta = 40$, $\bar{E_f} = 2000$ and $E_\infty = 0.5$.

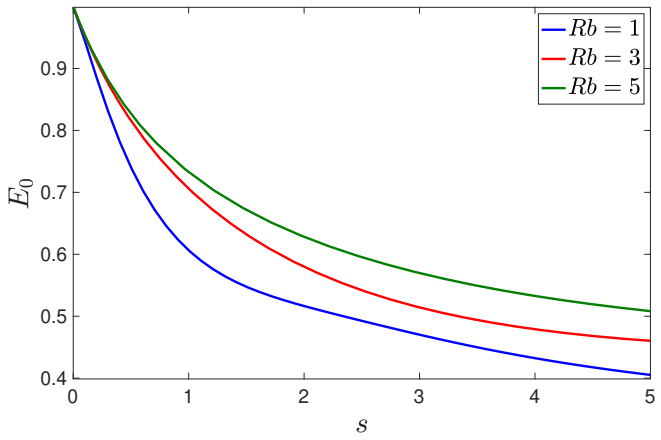

FIG. 8. Electric field versus arc length for different values of the Rossby number Rb. The other parameters are $We = 10$, $\bar{K} = 0.1$, $E_f = 200$, $\tilde{E}_f = 2000$, $\beta = 40$ and $E_\infty = 0.5$.

6. Temporal Instability Analysis

By considering small travelling wave modes about the steady state solutions of (4.23)-(5.5), which are solved in the previous section, we assume small perturbations as given by

$$(u,R,E,Q) = (u_0,R_0,E_0,Q_0)(s) + \delta(\hat{u},\hat{R},\hat{E},\hat{Q})\,exp(ik\bar{s}+\omega\bar{t}), \tag{6.1}$$

where $\bar{s} = s/\varepsilon$ and $\bar{t} = t/\varepsilon$ are small length and time scales, $k = k(s)$ and $\omega = \omega(s)$ are the wavenumber and frequency of the disturbances, and δ is a small constant which is $0 < \delta < \varepsilon^2$ (see Uddin (2007)). Replacing the leading order pressure term in equation (4.21) with the full curvature expression is necessary to avoid instability of wave modes with zero wavelength (see Eggers (1997)).

$$\begin{aligned} u_{0t} + u_0 u_{0s} = &-\frac{1}{We}\left(\frac{1}{R_0(1+R_{0s}^2)^{1/2}} - \frac{\varepsilon^2 R_{0ss}}{(1+R_{0s}^2)^{3/2}}\right)_s + \frac{(X+1)X_s + ZZ_s}{Rb^2} \\ &+\frac{3}{Re}\left(u_{0ss} + 2u_{0s}\frac{R_{0s}}{R}\right) + \tilde{E_f}\left(\frac{2}{R}Q_0E_0\right) + E_f\left(Q_0Q_{0s} + \beta E_0E_{0s}\right). \end{aligned} \tag{6.2}$$

The perturbation expansions (6.1) are now substituted into the equations (6.2), (4.22), (4.7) and (5.5), and we obtain the eigenvalue relation at leading order

$$\begin{aligned} &\left(\omega + iku_0\right)^3 + \left(\tfrac{3k^2}{\bar{Re}} + \tfrac{\bar{K}}{\sqrt{\beta}}\right)\left(\omega + iku_0\right)^2 \\ &-\left(\tfrac{k^2R_0}{2We}\left(\tfrac{1}{R_0^2} - k^2\right) - \tfrac{3k^2\bar{K}}{\bar{Re}\sqrt{\beta}} - \tfrac{E_f k^2 Q_0^2}{2} + E_f k^2 \beta E_0^2\right)\left(\omega + iku_0\right) \\ &-\left(\tfrac{k^2R_0\bar{K}}{2We\sqrt{\beta}}\left(\tfrac{1}{R_0^2} - k^2\right) + \tfrac{R_0 E_f k^2 \bar{K} Q_0^2}{2\sqrt{\beta}} + E_f k^2 \bar{K}\sqrt{\beta}E_0^2\right) = 0, \end{aligned} \tag{6.3}$$

where we have redefined $\bar{Re} = \varepsilon Re$ (see Alsharif et al. (2015) for a detailed discussion). We can notice that when there is no electric field in the problem, which means that $\bar{K} = Q_0 = E_0 = 0$, the eigenvalue

relation (6.3) becomes the eigenvalue relationship for Newtonian liquid jets that was found by Decent et al.(2009). In order to examine the behaviour of viscous curved fibers with an electric field, we use the dispersion relation (6.3). We note the large number of parameters in the equation which affect the mechanisms of the linear instability of this viscous curved fibres with the electric field, so we will keep some of them constant to simplify the analysis.

By solving (6.3) to find ω while assuming k to be real, we find regions of instability where $Re(\omega) > 0$. It is also of interest to find the maximum growth rate given by $Re(\omega_{max})$. A number of results are presented below for a range of parameters.

We show the relationship between the growth rate $Re(\omega)$, and the wavenumber k for different values of the electric force parameter E_f, and we notice that when we increase this non-dimensionless parameter, the growth rate increases (see Fig. 9). In Fig. 10, an increase in the dielectric constant ratio β leads to an increase in the growth rate and an increase in the range of unstable wavenumbers. The growth rate is also increasing when the Reynolds number is increased (see Fig. 11), but in that case the range of unstable wavenumbers does not change.

In Figs. 12 and 13, we have plotted the relationship between the maximum growth rate and different values of the electric force parameter E_f and the dielectric constant ratio β. From these graphs, we can see that by increasing β and E_f the maximum growth rate also increases. In Fig. 14, we can observe that an increase in the rotation rates (corresponding to Rb decreasing) leads to an increase in the maximum growth rate. In Figs. 15 and 16, we observe that by increasing the conductivity of the fluid $\bar{K}$ and the Reynolds number $\bar{Re}$, the maximum growth rate increases.

In the process of producing nanofibers is important to remove or minimize the beads developing on them. They correspond to instabilities, so it is important to find the best value for the parameters to avoid the instability or to reduce the maximum growth rate. We should also mention that (6.3) can be solved to find k for a given ω purely imaginary, which will be related to the spatial instability problem (see, for example, Decent et al. (2009) for curved viscous liquid jets).

7. Conclusion

In this study, the trajectory of a viscous liquid jet in centrifugal spinning under the influence of a radial electric field has been determined. It was shown that by decreasing the electric force parameter E_f and the rotation rate Rb the jet coils more, showing that the rotation rate and the electric field are affecting the trajectory of the jet. It is also shown that the surface charge increases more for high rotation rates along the jet, while the electric field decreases the jet radius. The temporal instability of a charged viscous liquid jet in centrifugal spinning has also been discussed. Moreover, we derived the dispersion relation needed to study the effects of the dimensionless parameters on the charged liquid curved jet. It has been found that increasing the dielectric constant ratio β leads to an increase in the growth rate. It is also observed that when we increase the conductivity of the fluid $\bar{K}$ and the Reynolds number $\bar{Re}$, the maximum growth rate increases.

The main industrial application of combining forcespinning and electrospinning is in the production of nanofibers from a variety of viscoelastic jets. However, the present study concentrates on the combined effect of centrifugal spinning and electrospinning on the trajectories and stability of liquid jets by considering the simpler case of Newtonian fluids. The results obtained here will be useful in future studies where concrete non-Newtonian liquid jets used in industrial applications and experiments to produce nanofibers will be investigated theoretically and numerically. In that case, for example, beads due to instability have been observed in experiments (e.g. Chang et al (2014)) and it is of interest to find

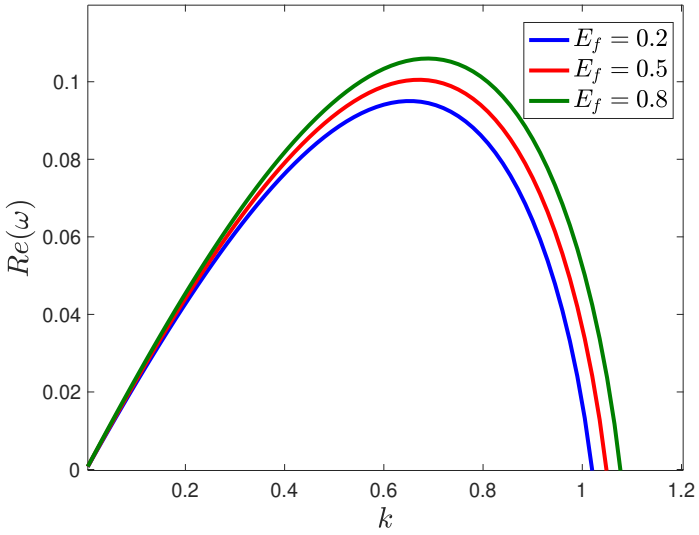

FIG. 9. $Re(\omega)$ versus k for different values of the electric force parameter E_f. The other parameters are $\bar{R}e = 30$, $We = 10$, $\bar{K} = 5$, and $\beta = 0.01$.

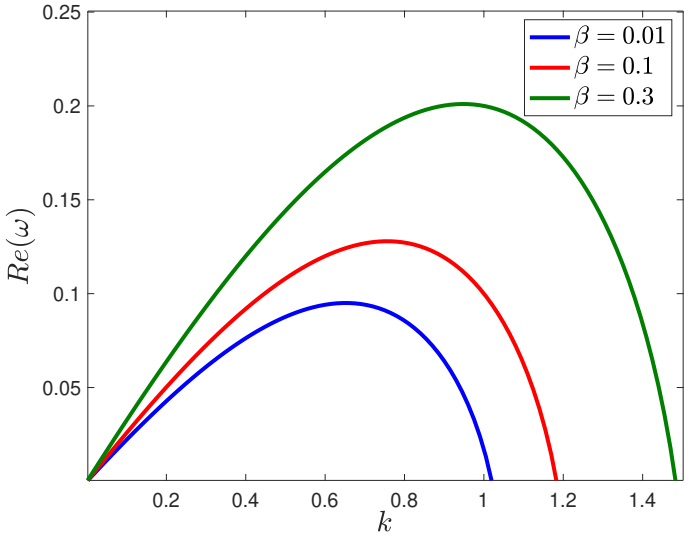

FIG. 10. $Re(\omega)$ versus k for different values of the dielectric constant ratio β. The other parameters are $\bar{R}e = 30$, $We = 10$, $\bar{K} = 5$, and $E_f = 0.2$.

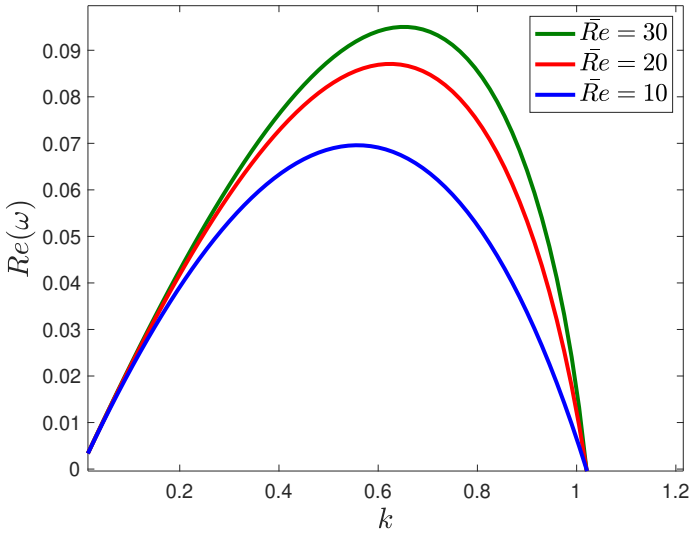

FIG. 11. $Re(\omega)$ versus k for different values of the Reynolds number $\bar{Re}$. The other parameters are $E_f = 0.2$, $We = 10$, $\bar{K} = 5$, and $\beta = 0.01$.

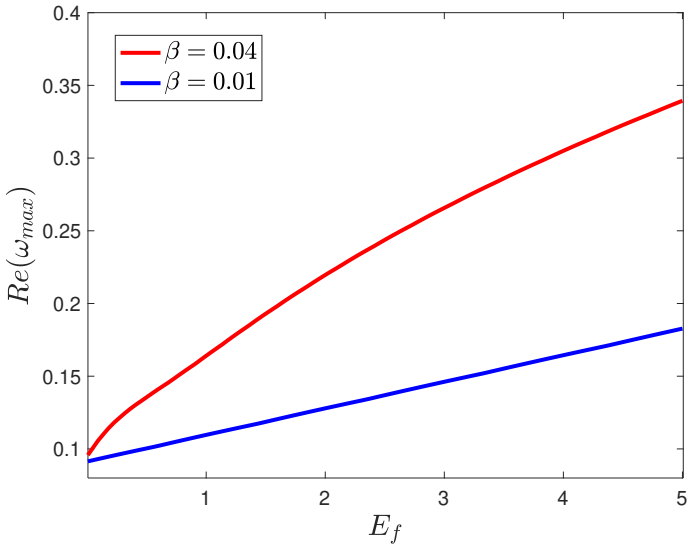

FIG. 12. $Re(\omega_{max})$ versus E_f for different values of the dielectric constant ratio β. At the nozzle $R_0 = E_0 = 1$ and $Q_0 = 0$, and the other parameters are $\bar{Re} = 30$, $We = 10$ and $\bar{K} = 0.1$.

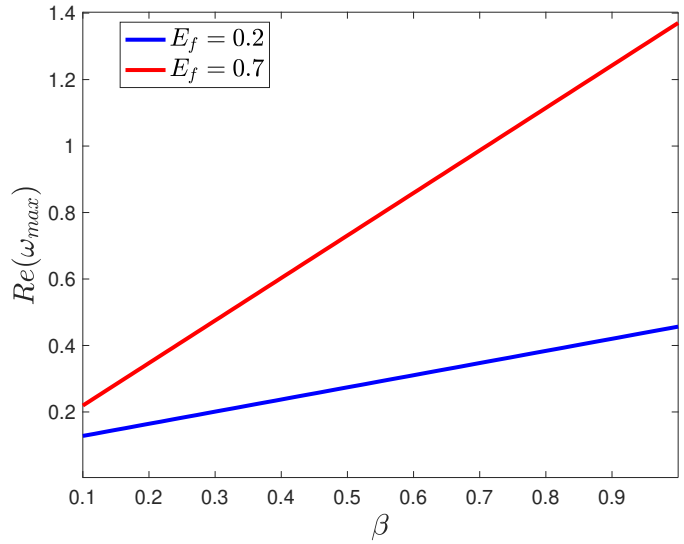

FIG. 13. $Re(\omega_{max})$ versus β for different values of electric field E_f. At the nozzle $R_0 = E_0 = 1$ and $Q_0 = 0$, and the other parameters are $\bar{R}e = 30$, $We = 10$ and $\bar{K} = 0.1$.

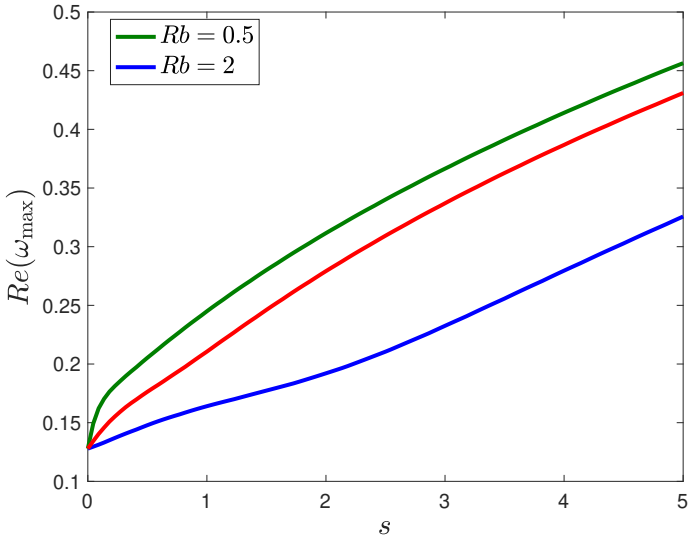

FIG. 14. $Re(\omega_{max})$ versus s for different values of the Rossby number Rb. The other parameters are $\bar{R}e = 30$, $We = 10$, $\bar{K} = 0.1$, $\beta = 0.1$ and $E_f = 0.2$.

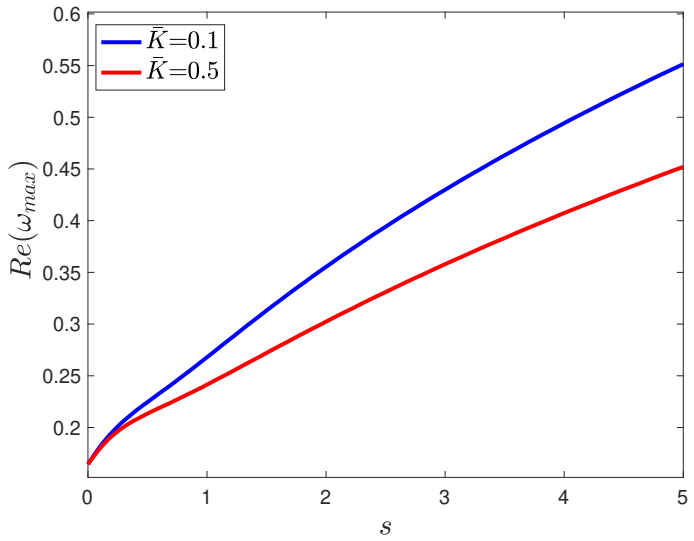

FIG. 15. $Re(\omega_{max})$ versus s for different values of the conductivity of the fluid $\bar{K}$. The other parameters are $\bar{Re} = 30$, $We = 10$, $\beta = 0.2$, $Rb = 1$ and $E_f = 0.2$.

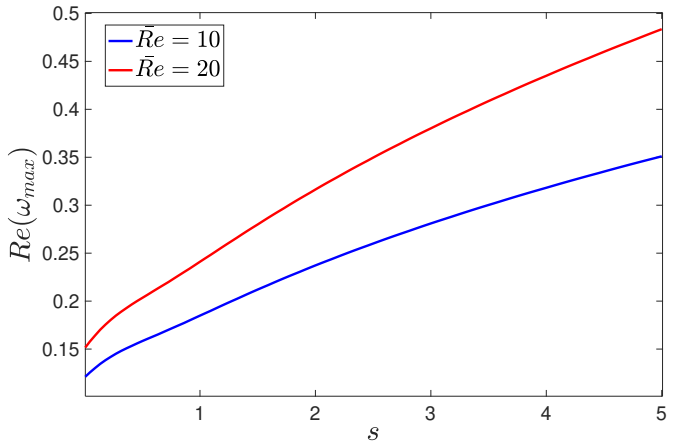

FIG. 16. $Re(\omega_{max})$ versus s for different values of the Reynolds number $\bar{Re}$. The other parameters are $We = 10$, $\bar{K} = 0.1$, $\beta = 0.2$, $Rb = 1$ and $E_f = 0.2$.

the regimes of parameters needed to avoid them.

The effect of surfactants on an electrospinning viscous liquid jet will also be examined for the future work, extending the methods developed by Alsharif and Uddin (2015) for a rotating non-Newtonian jet, but without an electric force. Another potential avenue of research is the study of spatial instability of curved liquid jets under the influence of centrifugal spinning and electrospinning.

Acknowledgments. Abdullah Alsharif would like to thank Taif University researchers supporting project number (TURSP-2020/96), Taif University, Taif, Saudi Arabia. The authors also thank Prof Mark Blyth (UEA) for some useful discussions about electric fields.

8. Appendix

Projecting the equations of motion (2.1) on our basis $(\mathbf{e_s}, \mathbf{e_n}, \mathbf{e}_\phi)$ we obtain

$$\frac{\partial u}{\partial s} + h_s \left(v + n \frac{\partial v}{\partial n} + \frac{\partial w}{\partial \phi} \right) + n \left(v \cos\phi - w \sin\phi \right) \left(X_s Z_{ss} - Z_s X_{ss} \right) = 0, \tag{8.1}$$

$$
\begin{aligned}
& h_s\left(\frac{\partial u}{\partial t}+(v\cos\phi-w\sin\phi)(Z_{st}X_s-X_{st}Z_s)+v\frac{\partial u}{\partial n}+\frac{w}{n}\frac{\partial u}{\partial\phi}\right)+u\frac{\partial u}{\partial s}+\\
& u(v\cos\phi-w\sin\phi)(X_sZ_{ss}-Z_sX_{ss})=-\frac{1}{\rho}\frac{\partial p}{\partial s}\\
& +\left(2\Omega(v\cos\phi-w\sin\phi)+\Omega^2((X+s_0)X_s+ZZ_s)\right)h_s\\
& +\frac{\mu}{\rho}\left(\frac{-n\cos\phi(X_sZ_{sss}-Z_sX_{sss})}{h_s^2}\left(\frac{\partial u}{\partial s}+v\cos\phi(X_sZ_{ss}-Z_sX_{ss})\right.\right.\\
& \left.-w\sin\phi(X_sZ_{ss}-Z_sX_{ss})\right)+\frac{1}{h_s}\left(-u(X_sZ_{ss}-Z_sX_{ss})^2+\frac{\partial^2 u}{\partial s^2}\right.\\
& +2\frac{\partial v}{\partial s}\cos\phi(X_sZ_{ss}-Z_sX_{ss})+v\cos\phi(X_sZ_{sss}-Z_sX_{sss})-w\sin\phi(X_sZ_{sss}-Z_sX_{sss})\\
& \left.-2\frac{\partial w}{\partial s}\sin\phi(X_sZ_{ss}-Z_sX_{ss})\right)+(1+2n\cos\phi(X_sZ_{ss}-Z_sX_{ss}))\frac{1}{n}\frac{\partial u}{\partial n}\\
& \left.+h_s\frac{\partial^2 u}{\partial n^2}+\frac{h_s}{n^2}\frac{\partial^2 u}{\partial\phi^2}-\frac{1}{n}\frac{\partial u}{\partial\phi}\sin\phi(X_sZ_{ss}-Z_sX_{ss})\right)+\frac{\varepsilon_1E_s}{\rho}\left[\frac{\partial E_s}{\partial s}+h_s\left(\frac{E_n}{n}+\frac{\partial E_n}{\partial n}\right)\right.\\
+\quad & \left.\cos\phi(X_sZ_{ss}-Z_sX_{ss})E_n+\frac{h_s}{n}\frac{\partial E_\phi}{\partial\phi}-E_\phi\sin\phi(X_sZ_{ss}-Z_sX_{ss})\right].
\end{aligned}
\tag{8.2}
$$

$$h_s\left(\frac{\partial v}{\partial t}+u\cos\phi\,(X_{st}Z_s-Z_{st}X_s)+v\frac{\partial v}{\partial n}+\frac{w}{n}\frac{\partial v}{\partial \phi}-\frac{w^2}{n}\right)+u\frac{\partial v}{\partial s}$$

$$-u^2\cos\phi\,(X_sZ_{ss}-X_{ss}Z_s)=-\frac{1}{\rho}\frac{\partial p}{\partial n}h_s-2\Omega h_s u\cos\phi$$

$$+(\Omega^2\cos\phi\,((X+s_0)Z_s-ZX_s+n\cos\phi))h_s$$

$$+\frac{\mu}{\rho}\left(\frac{-n\cos\phi\,(X_sZ_{sss}-X_{sss}Z_s)}{h_s^2}\left(\frac{\partial v}{\partial s}-u\cos\phi\,(X_sZ_{ss}-X_{ss}Z_s)\right)\right.$$

$$+\frac{1}{h_s}\left(-v\cos^2\phi\,(X_sZ_{ss}-X_{ss}Z_s)^2+\frac{\partial^2 v}{\partial s^2}-2\frac{\partial u}{\partial s}\cos\phi\,(X_sZ_{ss}-X_{ss}Z_s)\right.$$

$$\left.-u\cos\phi\,(X_sZsss-X_{sss}Z_s)+w\sin\phi\cos\phi\,(X_sZ_{ss}-X_{ss}Z_s)^2\right)$$

$$+(1+2n\cos\phi\,(X_sZ_{ss}-X_{ss}Z_s))\frac{1}{n}\frac{\partial v}{\partial n}+h_s\frac{\partial^2 v}{\partial n^2}-\frac{1}{n}(\frac{\partial v}{\partial \phi}-w)\sin\phi\,(X_sZ_{ss}-X_{ss}Z_s)+$$

$$\left.\frac{h_s}{n^2}(\frac{\partial^2 v}{\partial \phi^2}-v-2\frac{\partial w}{\partial \phi})\right)+\frac{\varepsilon_1 E_n}{\rho}\left[\frac{\partial E_s}{\partial s}+h_s\left(\frac{E_n}{n}+\frac{\partial E_n}{\partial n}\right)+\cos\phi\,(X_sZ_{ss}-Z_sX_{ss})E_n\right.$$

$$\left.+\frac{h_s}{n}\frac{\partial E_\phi}{\partial \phi}-E_\phi\sin\phi\,(X_sZ_{ss}-Z_sX_{ss})\right], \tag{8.3}$$

$$h_s\left(\frac{\partial w}{\partial t}+u\sin\phi(Z_{st}X_s-X_{st}Z_s)+v\frac{\partial w}{\partial n}+\frac{w}{n}\frac{\partial w}{\partial \phi}-\frac{vw}{n}\right)+u\frac{\partial w}{\partial s}+$$

$$u^2\sin\phi(X_sZ_{ss}-X_{ss}Z_s)=\left(-\frac{1}{\rho}\frac{1}{n}\frac{\partial p}{\partial \phi}h_s+2\Omega u\sin\phi+\right.$$

$$\left.\Omega^2\sin\phi(ZX_s-(X+s_0)Z_s-n\cos\phi)\right)h_s+$$

$$\frac{\mu}{\rho}\left(\frac{-n\cos\phi(X_sZ_{sss}-X_{sss}Z_s)}{h_s^2}\left(\frac{\partial w}{\partial s}+u\sin\phi(X_sZ_{ss}-X_{ss}Z_s)\right)+\right.$$

$$\frac{1}{h_s}\left(-w\sin^2\phi\,(X_sZ_{ss}-X_{ss}Z_s)^2+\frac{\partial^2 w}{\partial s^2}+2\frac{\partial u}{\partial s}\sin\phi\,(X_sZ_{ss}-X_{ss}Z_s)+\right.$$

$$\left.u\sin\phi(X_sZ_{sss}-X_{sss}Z_s)+v\sin\phi\cos\phi(X_sZ_{ss}-X_{ss}Z_s)^2\right)+$$

$$(1+2n\cos\phi(X_sZ_{ss}-X_{ss}Z_s))\frac{1}{n}\frac{\partial w}{\partial n}+h_s\frac{\partial^2 w}{\partial n^2}-(\frac{\partial w}{\partial \phi}+v)\sin\phi(X_sZ_{ss}-X_{ss}Z_s)+$$

$$\left.\frac{h_s}{n^2}(\frac{\partial^2 w}{\partial \phi^2}-w+2\frac{\partial v}{\partial \phi})\right)+\frac{\varepsilon_1 E_\phi}{\rho}\left[\frac{\partial E_s}{\partial s}+h_s\left(\frac{E_n}{n}+\frac{\partial E_n}{\partial n}\right)+\cos\phi(X_sZ_{ss}-Z_sX_{ss})E_n\right.$$

$$\left.+\frac{h_s}{n}\frac{\partial E_\phi}{\partial \phi}-E_\phi\sin\phi(X_sZ_{ss}-Z_sX_{ss})\right], \tag{8.4}$$

where $h_s=1+n\cos\phi(X_sZ_{ss}-X_{ss}Z_s)$.

After some algebra, the equations on our basis for the Gauss law and for the surface charge (2.2)-(2.3) are given by

$$\frac{1}{nh_s}\left\{n\frac{\partial E_s}{\partial s}+h_s\left(\frac{\partial(nE_n)}{\partial n}+\frac{\partial E_\phi}{\partial \phi}\right)+n\left(E_n\cos\phi-E_\phi\sin\phi\right)(X_sZ_{ss}-Z_sX_{ss})\right\}=\frac{q}{\varepsilon_1},, \tag{8.5}$$

$$\frac{\partial Q}{\partial t}+u\frac{1}{h_s}\cdot\frac{\partial Q}{\partial s}\left[1-\frac{1}{\Xi^2}\left(\frac{\partial R}{\partial s}\cdot\frac{1}{h_s}\right)^2\right]+v\frac{\partial Q}{\partial n}(1-\frac{1}{\Xi^2})+w\cdot\frac{1}{n}\cdot\frac{\partial Q}{\partial\phi}\left[1-\frac{1}{\Xi 2}\left(\frac{\partial R}{\partial\phi}\cdot\frac{1}{R}\right)^2\right]$$
$$-\frac{Q}{\Xi^2}\left\{\left(-\frac{\partial R}{\partial s}\right)\cdot\frac{1}{h_s^2}\left[\left(-\frac{\partial R}{\partial s}\right)\cdot\frac{1}{h_s^2}\left(\frac{\partial u}{\partial s}+\left(X_sZ_{ss}-X_{ss}Z_s\right)\left(u\cos\phi-u\sin\phi\right)\right)\right.$$
$$+\frac{\partial u}{\partial n}+\left(-\frac{\partial R}{\partial\phi}\right)\cdot\frac{1}{R}\cdot\frac{1}{n}\cdot\frac{\partial u}{\partial\phi}\Big]+\left(-\frac{\partial R}{\partial s}\right)\cdot\frac{1}{h_s^2}\left(\frac{\partial v}{\partial s}-\left(X_sZ_{ss}-X_{ss}Z_s\right)u\cos\phi+\frac{\partial v}{\partial n}\right)$$
$$+\left(-\frac{\partial R}{\partial\phi}\right)\cdot\frac{1}{R}\cdot\frac{1}{n}\left(\frac{\partial v}{\partial\phi}-w\right)+\left(-\frac{\partial R}{\partial\phi}\right)\cdot\frac{1}{R}\cdot\left[\left(-\frac{\partial R}{\partial s}\right)\cdot\frac{1}{h_s^2}\left(\frac{\partial w}{\partial s}+\left(X_sZ_{ss}-X_{ss}Z_s\right)\right.\right.$$
$$\left.\left.u\sin\phi+\frac{\partial w}{\partial n}+\left(-\frac{\partial R}{\partial\phi}\right)\cdot\frac{1}{R}\cdot\frac{1}{n}\left(\frac{\partial w}{\partial\phi}+v\right)\right]\right\}=\left[K_1\,\mathbf{E}\cdot\mathbf{n}\right]_2^1. \tag{8.6}$$

We can write the components of the stress tensor $\tau^{\mathbf{F}}$ in the curvilinear coordinate system as follows (see Wallwork (2002))

$$\tau_{11}^F=\frac{1}{h_1}\frac{\partial u_1}{\partial\xi_1}+\frac{u_2}{h_1h_2}\frac{\partial h_1}{\partial\xi_2}+\frac{u_3}{h_3h_2}\frac{\partial h_1}{\partial\xi_3},$$

$$\tau_{23}^F=\frac{h_3}{2h_2}\frac{\partial}{\partial\xi_2}\left(\frac{u_3}{h_3}\right)+\frac{h_2}{2h_3}\frac{\partial}{\partial\xi_3}\left(\frac{u_2}{h_2}\right).$$

Here, we have chosen $\xi_1=s$, $\xi_2=n$, $\xi_3=\phi$ and $h_1=h_s,h_2=1,h_3=n$.

$$\tau_{ss}^F=-p+2\mu.\frac{1}{h_s}.\left[\frac{\partial u}{\partial s}+(\upsilon\cos\phi-w\sin\phi)(X_sZ_{ss}-X_{ss}Z_s)\right],$$

$$\tau_{nn}^F=-p+2\mu\,\frac{\partial\upsilon}{\partial n},$$

$$\tau_{\phi\phi}^F=-p+2\mu.\frac{1}{n}.\left(\frac{\partial w}{\partial\phi}+\upsilon\right),$$

$$\tau_{sn}^F=\mu\left[\frac{1}{h_s}\frac{\partial\upsilon}{\partial s}+\frac{\partial u}{\partial n}-\frac{u}{h_s}\cos\phi(X_sZ_{ss}-X_{ss}Z_s)\right],$$

$$\tau_{n\phi}^F=\mu\left(\frac{\partial w}{\partial n}-\frac{w}{n}+\frac{1}{n}.\frac{\partial\upsilon}{\partial\phi}\right)$$

and

$$\tau_{s\phi}^F=\mu\left[\frac{1}{n}.\frac{\partial u}{\partial\phi}+\frac{u}{h_s}\sin\phi(X_sZ_{ss}-X_{ss}Z_s)+\frac{1}{h_s}.\frac{\partial w}{\partial s}\right].$$

REFERENCES

ALSHARIF, A. M., UDDIN, J. AND AFZAAL, M. F., (2015) Instability of viscoelastic curved jets., *Appl. Math. Modell.* **39**, 3924-3938.

ALSHARIF, A. M. AND UDDIN, J., (2015) Instability of viscoelastic curved jets with surfactants., *Journal of Non-Newtonian Fluid Mechanics* **216**, 1-12.

ALSHARIF, A. M.,(2019) Instability of non-Newtonian liquid jets in centrifugal spinning with surfactants, *Fluid Dynamics Research* **51(3)**, 035510.

CHANG, W. M., WANG, C. C., AND CHEN, C. Y., (2014) The combination of electrospinning and forcespinning: Effects on a viscoelastic jet and a single nanofiber. *Chemical Engineering Journal,* **244**, 540-551.

DABIRIAN, F., RAVANDI, S. H., AND PISHEVAR, A. (2013) The effects of operating parameters on the fabrication of polyacrylonitrile nanofibers in electro-centrifuge spinning. *Fibers Polym.* **14(9)**, 1497-1504.

DECENT, S. P., KING, A. C. AND WALLWORK, I. M., (2002) Free jets spun from a prilling tower, *Journal of Engineering Mathematics* **42**, 265-282.

DECENT, S. P., KING, A. C., SIMMONS, M. H., PĂRĂU, E. I., WONG, D. C. Y., WALLWORK, I. M., GURNEY, C., AND UDDIN, J., (2009) The trajectory and stability of a spiralling liquid jet: Part II. Viscous Theory. *Appl. Math. Modelling,* **33 (12),** 4283-4302.

DECENT, S. P., PĂRĂU, E. I., SIMMONS M. J. H. AND UDDIN, J., (2018) On mathematical approaches to modelling slender liquid jets with a curved trajectory. *Journal of Fluid Mechanics* **844,** 905-916.

DIVVELA, M. J., RUO, A., ZHMAYEV. Y. AND JOO, Y. L., (2017) Discretized modeling for centrifugal spinning of viscoelastic liquids. *Journal of Non-Newtonian Fluid Mechanics,* **247,** 62-77.

DOSHI, J. AND RENEKER, D. H., (1993,) Electrospinning process and applications of electrospun fibers, *Ind. Appl. Soc. Ann. Meet.* **3**,1698-1703.

EGGERS, J. (1997) Nonlinear dynamics and breakup of free surface flows. *Rev. Mod. Physis,* **69, (3),** 865-929.

EGGERS, J. G. (2008). Physics of liquid jets. *Reports on progress in Physics*, **71**, 3, 036601 - 036679.

HOHMAN, M. M., SHIN, M., RUTLEDGE, G. ABD BRENNER, M. P. 1984, Electro- spinning and electrically forced jets. II. Application. *Phys. Fluids,* **13, 8,** 2221-2236.

FENG, J.J., (2002) The stretching of an electrified non- Newtonian jet: A model for electrospinning. *Phys Fluids* **14**, 3912.

FENG, J.J., (2003) Stretching of a straight electrically charged viscoelastic jet. *J. Non-Newtonian Fluid Mech.* **116 (1),** 55-70.

HASHEMI, A.R., PISHEVAR, A. R., VALIPOURI, A. AND PĂRĂU, E.I. (2018) Numerical and experimental study on the steady cone-jet mode of electro-centrifugal spinning, *Phys. Fluids* **30**, 017103.

HAWKINS, V. L., GURNEY, C. J., DECENT, S. P., SIMMON, M. J. H. AND UDDIN, J., (2010) Unstable waves on a curved non-Newtonian liquid jet. *J. Phys. A: Math. Theor.* **43**, 055501.

HOHMAN, M. M., SHIN, M. RUTLEDGE, G. AND BRENNER M. P.,(2001) Electrospinning and electrically forced jets: I. Stability theory, *Phys. Fluids* **13,** 2201-2220.

HOHMAN, M. M, SHIN, M.,RUTLEDGE, G. AND BRENNER, M.P., (2001) Electrospinning and electrically forced jets: II. Applications. *Phys. Fluids* **13** 2221-2236.

JONES, A.R. AND THONG, K.C., (1971) The production of charged monodisperse fuel droplets by electrical dispersion. *J. Phys. D: Apps. Phys.* **4,** 1159-1166.

LIAO, C. C., WANG, C. C., AND CHEN, C. Y.,LAI, W. J. (2011) Stretching-induced orientation of polyacrylonitrile nanofibers by an electrically rotating viscoelastic jet for improving the mechanical properties. *Polymer* **52 (10),** 2263-2275.

LIAO, C. C., WANG, C. C., AND CHEN, C. Y., (2011) Stretching-induced crystallinity and orientation of polylactic acid nanofibers with improved mechanical properties using an electrically charged rotating viscoelastic jet. *Polymer,* **52(19),** 4303-4318.

NOROOZI, S., ALAMDARI, H., ARNE, W., LARSON, R. G., TAGHAVI, S. M., (2017) Regularized string model

for nanofibre formation in centrifugal spinning methods. *J. Fluid. Mech.,* **822,** 202-234.

PAPAGEORGIOU, D. T., (2019) Film flows in the presence of electric fields. *Annual Review of Fluid Mechanics* **51,** 155-187.

PĂRĂU, E. I., DECENT, S. P., SIMMONS, M. J. H., WONG, D. C. Y. AND KING, A. C., (2006) Nonlinear travelling waves on a spiralling liquid jet, *Wave Motion*, **43**, 599-618.

PĂRĂU, E. I., DECENT, S. P., SIMMONS, M. J. H., WONG, D. C. Y. AND KING, A. C., (2007) Nonlinear viscous liquid jets from a rotating orifice. *J. of Eng. Maths.,* **57**, 159-179.

PARTRIDGE, L., WONG, D. C. Y., SIMMONS, M. J. H., PĂRĂU, E. I., AND DECENT, S. P., (2005) Experimental and theoretical description of the break-up of curved liquid jets in the prilling process. *Chem. Eng. Res. Des.* **83(A11)** 1267- 1275.

RAYLEIGH, W. S., (1878) On the instability of jets. *Proc. Lond. Math. Soc.* **10**,4.

RENARDY, M., (1995) A numerical study of the asymptotic evolution and breakup of Newtonian and viscoelastic jets. *J. Non-Newtonian Fluid Mech.,* **59**, 267-282.

RENEKER, D. H., YARIN, A. L., FONG, H. AND KOOMBHONGSE S., (2000) Bending instability of electrically charged liquid jets of polymer solutions in electrospinning. *J. Appl. Phys.* **87**, 4531-4547.

RIAHI, D. N., (2017) Modeling and computation of nonlinear rotating polymeric jets during force spinning process. *International Journal of Non- linear Mechanics,* **92**,1-7.

RIAHI, D. A., (2019) On nonlinear rotating electrified non-Newtonian jets. *International Journal of Non-Linear Mechanics* **109**, 166-171.

ROGALSKI J J, BASTIAANSEN C W M AND PEIJS T, (2017) Rotary jet spinning review a potential high yield future for polymer nanofibers. *Nanocomposites*, **3(4)**, 97-121.

SAVILLE, D. A., (1997) Electrohydrodynamics: the Taylor-Melcher leaky dielectric model. *Annual review of fluid mechanics,* **29**, 27-64.

SHIN,Y. M., HOHMAN, M.M., BRENNER, M.P. AND RUTLEDGE, G.C., (2001) Electrospinning: A whipping fluid jet generates submicron polymer fibers, *Appl. Phys. Lett.* **78**, 1149-1151.

SPIVAK, A. F. AND DZENIS, Y. A.. (1998) Asymptotic decay of radius of a weakly conductive viscous jet in an external electric field, *Appl. Phys. Lett.* **73**, 3067.

STONE, H. A., LISTER, J. R., AND BRENNER, M. P., (1999) Drops with conical ends in electric and magnetic fields, *Proc. R. Soc. Lond. A,* **455,** 329-347.

TAGHAVI, S. M. AND LARSON, R. G., (2014) Regularized thin-fiber model for nanofiber formation by centrifugal spinning, *Physical Review E,* **89 (2)**, 023011.

MELCHER, J. R., AND TAYLOR, G.I., (1969) Electrohydrodynamics: a review of the role of interfacial shear stresses, *Annual review of fluid mechanics* **1**, 111-146.

TOMITA, Y., ISHIBASHI, I. AND YOKOYAMA, T., (1986) Fundamental studies on an electrostatic ink jet printer: 1st report, electrostatic drop formation,*Bull. Japan Soc. Mech. Eng.* **29**, 3737-3743.

UDDIN, J., (2007) An investigation into methods to control breakup and droplet formation in single and compound liquid jets, *Ph.D. thesis, University of Birmingham*, Birmingham, UK.

YARIN, A.,(1993), *Free Liquid Jets and Films: Hydrodynamics and Rheology*, Longman, Harlow, and Wiley, New York.

YARIN, A. L. KOOMBHONGSE, S., AND RENEKER, D. H., (2001) Bending instability in electrospinning of nanofibers, *J. Appl. Phys.* **89**, 3018-3026.

WALLWORK I. M., (2002) The trajectory and stability of a spiralling liquid jet, *PhD Thesis, University of Birmingham*, Birmingham, UK.

WALLWORK, I. M., DECENT, S. P., KING, A. C., AND SCHULKES, R. M. S. M. (2002) The trajectory and stability of a spiralling liquid jet. Part 1. Inviscid theory, *J. Fluid Mech.* ***459****, 43-65.*

WEBER, C., *(1931) Zum Zerfall eines Flussigkeitsstrahles.* Z. Angew. Math. Mech, ***11****, 136-154.*

WONG, D. C. Y., SIMMONS, M. J. H., DECENT, S. P., PĂRĂU, E. I. AND KING, A. C. *(2004) Break-up dynamics and drop sizes distributions created from spiralling liquid jets,* International Journal of Multiphase

Flow, ***30,*** *5, 499-520.*